

# Relations between Molecular, Crystalline, and Lamellar Structures of Amylopectin

Torsten Witt,<sup>†,‡</sup> James Douth,<sup>§</sup> Elliot P. Gilbert,<sup>§</sup> and Robert G. Gilbert<sup>\*,†,‡</sup>

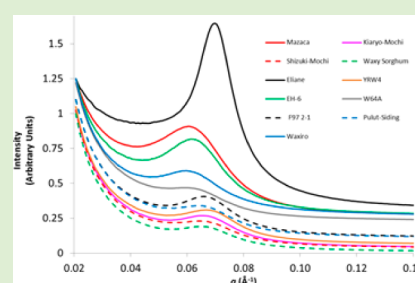
<sup>†</sup>Tongji School of Pharmacy, Huazhong University of Science and Technology, Wuhan, China, 430030

<sup>‡</sup>Centre for Nutrition and Food Science, Queensland Alliance for Agriculture and Food Innovation, The University of Queensland, Brisbane, Qld 4072, Australia

<sup>§</sup>Bragg Institute, Australian Nuclear Science and Technology Organisation, Locked Bag 2001, Kirrawee DC, NSW 2232, Australia

**S** Supporting Information

**ABSTRACT:** Chain (branch) length distributions (CLD) from size-exclusion chromatography of a series of waxy starches were parametrized using both an empirical and a biosynthesis-based method and correlated with their crystalline–amorphous lamellar properties obtained from X-ray scattering. Correlations were best seen with the biosynthesis-based parametrization. This showed for the first time that the following links between the CLD and lamellar parameters, the average interlamellar repeat distance and the distribution of these distances, were decreased by an increase in the proportion of very short branches and were increased by an increase in the proportion of intermediate and longer chains; further, the shoulder and linear sections of the CLD were found to affect the lamellar repeat distance and distribution. These effects are rationalized in terms of branch-length effects on the production of crystallites and the presence of portions of longer branches in the amorphous regions.



## INTRODUCTION

Starch is a branched homopolymer of glucose separated into two broad categories of macromolecules, amylose and amylopectin, wherein the glucose monomers have  $\alpha$ -(1 $\rightarrow$ 4) linear bonds and  $\alpha$ -(1 $\rightarrow$ 6) branch points. Amylose displays a low degree of branching, high average chain length, and low average macromolecular size (and molecular weight); amylopectin macromolecules have a high degree of branching, low average chain length, and high average macromolecular size (and molecular weight). Starch has a complex multilevel structure, but there is limited understanding as to how and to what extent the structure at a lower level controls that at a higher. These levels can be grouped as follows. The lengths of the individual chains that form the starch branches is the lowest (level 1), with the next level being the branching structure (level 2). The inter- and intramolecular aggregations that starch chains undergo in the native state during biosynthesis comprise level 3. Finally, the highest levels are those of growth rings and the macroscopic granular structure.

For the intermediate levels, branches aggregate to form either single or double helices of varying lengths. The single helices can form V-type crystallites, while the double helices can produce A- or B-type crystallites. V-type crystallites can be due to a variety of different crystal unit cells, depending on the nature of the molecule with which the starch chain complexes to produce the crystallites;<sup>1</sup> in nature, the complexing agent is typically some form of lipid.<sup>2</sup> A-type crystallites have a monoclinic unit cell<sup>3,4</sup> and the B-type crystallites a hexagonal unit cell that contains a large water channel.<sup>5,6</sup> C-type crystallinity is a mixture of both A- and B-type crystallites.<sup>7</sup> Both A- and B-type crystallites

can undergo further aggregation to form crystalline–amorphous lamellae with an average repeat distance of 8.5–10 nm; this is conserved in all starch-producing species.<sup>8,9</sup> Information on this lamellar structure can be obtained through small-angle scattering data, interpreted using a number of different fitting models.<sup>10–15</sup> While the limits of the average repeat distance of the crystalline–amorphous lamella is highly conserved, there is significant variability between specific starches and species.<sup>11,16–18</sup>

The formation of higher-order starch granular structures is not wholly determined by the molecular structure of isolated starch molecules: for example, granular structure and much crystallinity are lost upon solvation or gelatinization and then removal of solvent or swelling agent.<sup>10</sup> Additionally, annealing can be used to lower the free energy of starch<sup>19</sup> or to change its crystal structure and type.<sup>20</sup> Thus, higher structural levels are influenced by kinetic effects: for example, as starch branches are produced, they may aggregate rapidly with aggregation being modified by conditions present in the amyloplast, and may be “shepherded” by biosynthetic enzymes, producing a structure that, although stable, is not at the absolute free-energy minimum.

The objective of the present paper is to see to what extent causally reasonable correlations can be found between the lowest structural level, the chain-length distribution (CLD), and the higher-level structural features based on crystallinity in the native starch. This analysis requires expressing the CLD in terms of a manageable number of parameters. There are three methods

**Received:** October 13, 2012

**Revised:** November 13, 2012

**Published:** November 14, 2012

currently in use. (1) Difference plots are useful to reveal broad qualitative differences between dissimilar starches and have been used extensively and successfully to correlate the effects of different starch synthesis enzymes. However, this approach is not useful in reducing the CLD into a small number of meaningful parameters.<sup>21</sup> (2) The division of the CLD into different regions and observing their effect has been used to explore and explain a variety of processing effects such as pasting and gelatinization properties,<sup>22,23</sup> freeze–thaw stability,<sup>24</sup> and differences in the thermal stability of crystallites.<sup>25</sup> The method of division used by Hanashiro et al.<sup>26</sup> is the most frequently used and, as employed here, is denoted “Subdivision Analysis”. (3) A recent model for starch biosynthesis by Wu and Gilbert<sup>21</sup> enables the CLD to be expressed in a small number of parameters expressing the relative activities of the various enzymes involved; this is termed here “Biosynthesis-Based Analysis”. In principle, this model contains all the information that is found within the difference plots and the CLD proportional separations; however, the comparison of the parameters produced by the model will not necessarily produce clearer causal links controlling higher-level structure than the other methods. These different parametrization methods can be seen as complementary, as they encapsulate the CLD in different ways.

The current work aims to provide a more accurate and comprehensive observation of the effect of the branch structure (level 1) of amylopectin and the aggregation of the branches into the higher-ordered structures and the way those higher-level structures interact (level 3). The work will focus on waxy starches from both the same and different botanical lines so as to provide a wide range of structures. A more thorough understanding of these influences will begin to allow an understanding of which native starch structures are wholly defined by their molecular parameters and which are more related to kinetics or biology.

## EXPERIMENTAL SECTION

**Starch Samples.** A total of 11 waxy starch samples from rice, maize, wheat, and barley were selected and are listed in the Supporting Information (Table S19). All grains were hand-ground in a mortar and pestle, loose material removed, and samples passed through a 250  $\mu\text{m}$  sieve. The starch was purified using the following method. A total of 3 g flour was incubated with 15 mL of 34  $\text{mg L}^{-1}$  P6887-5g Pepsin from porcine gastric mucosa (Sigma) in 0.01 M sodium acetate buffer (pH 3.5) at 37  $^{\circ}\text{C}$  for 1 h. After incubation, the flours were precipitated with 35 mL of ethanol and centrifuged at 3000  $g$  for 5 min in a Beckman-Coulter Avanti J-E Centrifuge (Beckman-Coulter Australia, Gladesville, Australia), the supernatant discarded, and the pellet resuspended in 35 mL of ethanol. The sample then underwent the same centrifugation and resuspension a total of three times. The pellet was then suspended in acetone and centrifuged at 3000  $g$  for 5 min three times, after which the pellet was allowed to air-dry overnight and then stored.

**Size Exclusion Chromatography.** Prior to size separation, the starch samples were debranched to characterize the separate starch chains, following a procedure detailed in Hasjim et al.<sup>27</sup> Universal calibration and data manipulation with relation to the SEC differential refractive index (DRI) signal were conducted as detailed elsewhere,<sup>28–30</sup> including the relation between elution volume, hydrodynamic volume  $V_h$  (and the corresponding hydrodynamic radius  $R_h$ ), and degree of polymerization (abbreviation DP, symbol  $X$ ) of linear chains (following SEC characterization after debranching).

The proportion of amylose was determined by integrating the debranched SEC weight distribution  $w_{\text{de}}(\log R_h)$  for the branches that correspond to amylopectin ( $\log(R_h/\text{nm}) \leq 0.65$ ) and amylose ( $\log(R_h/\text{nm}) > 0.65$ ).<sup>29,31</sup> An example of this plot is given in Figure 1.

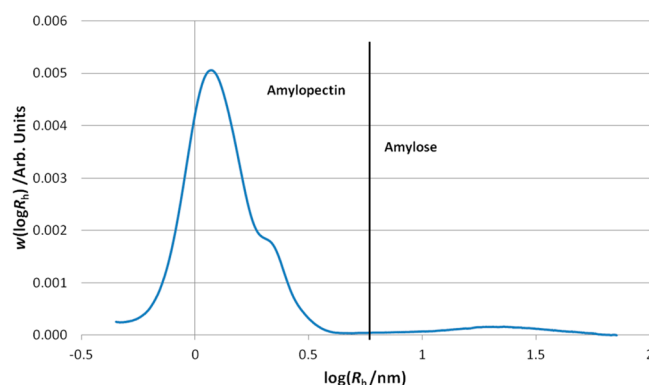


**Figure 1.** Weight distribution of YRW4 branches obtained using SEC. The vertical line divides the amylose and amylopectin regions.

This debranched weight distribution,  $w(\log R_h)$ , is converted to the corresponding number distribution,  $N_{\text{de}}(X)$ , using the relation

$$w(\log R_h) = X^2 N_{\text{de}}(X) \quad (1)$$

which is valid only for linear polymers. The dependence of DP  $X$  on size  $R_h$  is found from the Mark–Houwink equation and measured Mark–Houwink parameters. The CLD of the amylopectin chains was parametrized using two methods as follows. (1) The number distribution was separated into four categories:  $X = 6–12$ ,  $13–22$ ,  $25–36$ , and  $\geq 37$  and described as short, medium, long, and very long, respectively, with the area under the curve determined as developed by Hanashiro et al.<sup>26</sup> (2) The number distribution was also fitted using the Wu–Gilbert model, which considers the CLD from a biosynthetic perspective. In this model, the number distribution is assumed to be controlled solely by the action of three types of starch biosynthesis enzyme: starch synthase, starch branching enzyme, and starch debranching enzyme. The kinetic equations of the rates of action of each enzyme determine the number distribution of branches, that is,  $N_{\text{de}}(X)$ , giving the relative number of chains of the debranched starched comprising  $X$  monomer units. There are several different sets of the three types of enzymes, denoted “enzyme sets”: for example, there are four isoforms of branching enzyme, SBEI, SBEII, SBEIIa and SBEIIb, and a particular enzyme set contains only one of these four (plus one each of the various types of starch synthase and debranching enzymes). The overall  $N_{\text{de}}(X)$  is the sum of the contributions of each enzyme set. The mathematical treatment shows that  $N_{\text{de}}(X)$  is given entirely by a small number of parameters, divided into two categories. (i) The first category of parameter comprises the relative contributions of each enzyme set; for example, “2/1” represents the relative contribution of enzyme set 2 to that of set 1. (ii) The second category comprises the ratio of the rates (enzyme activity) of starch branching enzyme to that of starch synthase, this parameter being denoted  $\beta$ , and two minimum-DP parameters, denoted  $X_0$  and  $X_{\text{min}}$ .  $X_0$  is the minimum DP of the remnant chain left when branching enzyme breaks off the end of the chain to form a new branch, and  $X_{\text{min}}$  is the minimum DP of the chain that has been broken off. It is found for the first enzyme set that typical values of the minimum-DP parameters are  $X_{\text{min}} \sim 10$  and  $X_0 \sim 4$ . The rather complicated mathematical dependence of  $N_{\text{de}}(X)$  on  $\beta$ ,  $X_0$  and  $X_{\text{min}}$  are given in the Wu–Gilbert paper.<sup>21</sup>

The source of the number distributions here is size exclusion chromatography (SEC). Although fluorophore-assisted capillary electrophoresis data<sup>32</sup> would be more accurate for smaller chains, this technique cannot detect the longest ones, which are however accurately obtained from SEC. On the other hand, SEC suffers from band broadening, which masks fine structure in the CLD. This precludes the use of more than two enzyme sets here. The parameters from fitting these data comprise the following: (a) for each of the two enzyme sets considered here, the ratios of the activities of starch branching enzyme to that of starch synthase,  $\beta_1$  and  $\beta_2$  (which produce a steeper slope in the linear sections of the CLD with increasing  $\beta$ ); (b) the minimum DPs of the snipped moiety for the branching enzyme to operate  $X_{\text{min}1}$  and  $X_{\text{min}2}$ , respectively

(which increase the length of the peak and shoulder regions with increasing  $X_{\min}$ ); and (c) the relative contributions of enzyme set 2 to that of set 1, denoted 2/1.  $X_{01}$  was assigned the value of 4 and  $X_{02}$  was assigned the value of 1 throughout, as found by Wu and Gilbert. The nonlinear least-squares fitting procedure used to fit an experimental  $N_{de}(X)$  is given in detail in the Wu–Gilbert paper.<sup>21</sup> A typical fit of Kiaryo–Mochi with the contribution of both isoforms is shown in Figure 2, with all other replicate data presented in the Supporting Information (SI).

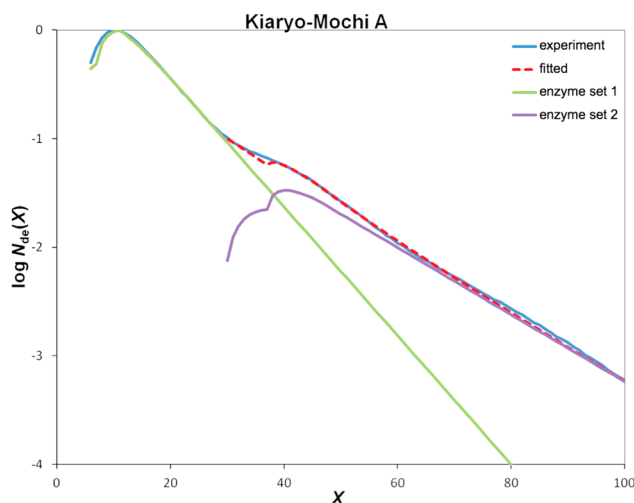


**Figure 2.** Plot of the experimental results from SEC (in blue) and the model fitting (in red) of the Kiaryo–Mochi starch. The total CLD,  $N_{de}(X)$ , is the sum of the components from enzyme sets 1 and 2 (green and purple, respectively); note that the plot has a logarithmic scale, as  $\log N_{de}(X)$ .

**<sup>1</sup>H NMR.** Sample preparation for <sup>1</sup>H NMR was conducted following Tizzoti et al.<sup>33</sup> The starch sample, dissolved in DMSO-*d*<sub>6</sub> (Sigma, Castle Hill, NSW Australia)–TFA-*d*<sub>1</sub> (Sigma, Castle Hill, NSW Australia) solution, was transferred to a 5 mm NMR tube. The NMR spectra were measured on a Bruker Avance NMR spectrometer operating at a Larmor frequency of 500.13 MHz for <sup>1</sup>H equipped with a TXISz probe (Bruker Biospin). An 8 μs 90° pulse is used with a repetition time of 15.07 s, which is composed of a 3.07 s acquisition time and a relaxation delay of 12 s. The experiment is run at 70 °C with 172 scans; this number of scans was chosen as there was minimal change to the ratio of α-(1→4) to α-(1→6) bonds after 164 scans. A total of 45 min was allowed for the sample to become stable within the spectrometer before any scans were performed. The method to obtain the degree of branching is found in Tizzotti et al.<sup>33</sup>

**X-ray Diffraction.** X-ray diffraction experiments were performed on a PANalytical (Almelo, The Netherlands) XPert Pro multipurpose diffractometer. The equipment used a copper long fine focus tube with incident beam divergence slit and diffracted beam scatter slit fixed at 0.125° and an X'celerator high speed detector. The samples were observed over the angular range of 4–35°, with a step size of 0.0334° and a count time of 220 s per point. Approximately 2 g of starch was used per sample, resulting in a sample depth of 4 mm. The data were analyzed using Systat PeakFit v. 4.12 (Systat, San Jose, U.S.A.), which employs a Levenberg–Marquardt nonlinear minimization algorithm for peak fitting. The percentage of the total scattering due to crystalline and amorphous starch, as well as the relative proportions of A-, B-, and V-type crystallinity, was found by the Lopez–Rubio et al. fitting method.<sup>34</sup>

**Small Angle X-ray Scattering (SAXS).** Small angle X-ray scattering measurements were taken using a Bruker NanoStar SAXS camera, with pinhole collimation for point focus geometry using a wavelength of 1.54 Å (Cu K<sub>α</sub>). Details of the experimental set up can be found in Blazek et al.<sup>35</sup> Starch powders as hydrated slurries were presented to the X-ray beam in 2 mm quartz capillaries (Hilgenburg GmbH,

Germany). A background measurement of quartz capillary filled with water was subtracted from the starch data after correction for transmission. The data were reduced to absolute scale using liquid water as a standard following the method of Fan et al.<sup>36</sup> These operations were performed using the IRENA macro suite for manipulating and analyzing small-angle scattering data<sup>37</sup> within Igor (Wavemetrics, Lake Oswego, Oregon). SAXS data were fitted empirically using a power law function to represent the low-*q* scattering region and a Lorentzian to represent the crystalline–amorphous lamella peak. This approach allows the production of values which represent the peak height, the peak center position (the average repeat distance of the crystalline–amorphous lamella), and the half width at half-maximum (HWHM, a reciprocal-space quantity giving an indication of the polydispersity of the crystalline–amorphous lamella), through eq 2.<sup>18</sup>

$$I(q) = Aq^{-\delta} + I_0 \left( 1 + \frac{q - q_0}{B^2} \right)^{-1} + \beta \quad (2)$$

Here  $A$  is the power law prefactor,  $\delta$  is the power law decay,  $I_0$  is the height of the peak,  $B$  is the lamellar HWHM (units Å<sup>−1</sup>),  $q_0$  is the position of the Lorentzian peak (also in reciprocal space units), and  $\beta$  is the background. Data fitting was performed using least-squares refinement in the NCNR analysis macros.<sup>11,38</sup> The average lamellar repeat distance is related to  $q_0$  by eq 3, and reciprocal-space HWHM, which is converted to real space using eq 4.

$$\text{average repeat distance (real space)} = \frac{2\pi}{q_0} \quad (3)$$

$$\text{HWHM (real space)} = \frac{2\pi B}{q_0^2} \quad (4)$$

The scattering intensity of the starch samples not only varies between the different starches, but also between different replicates of the same starch. This is partly due to uncertainty of, and inability to control significantly, the packing density during sample preparation. Such variations in scattering intensity preclude the possibility of drawing conclusions between samples based on lamellar peak height.

**Statistics.** Pearson correlation coefficients were used to suggest linear correlations between the following parameters: degree of branching (from NMR), and, from the debranched SEC data, proportions of short, medium, long, and very amylopectin branches (using the method of Hanashiro et al.<sup>26</sup>),  $\beta_1$ ,  $\beta_2$  (which are the activity ratios for the two enzyme sets considered), ratio of the contributions to the overall CLD from the two enzyme sets (denoted 2/1), proportion of amylose, average crystalline–amorphous lamellar repeat distance, HWHM of crystalline–amorphous lamellae, proportion of A- or B-type crystallinity, and proportion of V-type crystallites. Correlation coefficients  $p < 0.05$  were taken as statistically significant and  $0.05 < p \leq 0.1$  as possibly significant. Spearman correlation coefficients were used to identify if there were any nonlinear correlations; this information can be found in the SI.

## RESULTS AND DISCUSSION

The structural parameters of the CLD studied in this work are presented in Table 1. The degree of branching is equal to the reciprocal of the first moment of the number distribution, so it is, in principle, possible to determine the degree of branching from the SEC CLD. However, the number distribution data obtained from SEC suffer from band broadening and sensitivity to calibration; as neither of these occurs in <sup>1</sup>H NMR, the NMR values are more accurate. A comparison between the results for the degree of branching obtained by NMR and SEC is given in the SI. The values for the proportion of amylose as determined by debranched SEC is typically low for all of the waxy starches (below 3%), except Waxiro barley starch, which had a significantly greater proportion of amylose (~10%).

**Subdivision Analysis.** The difference plots of the number distributions from debranched SEC are presented in Figure 3



Table 1. Levels 1 and 3 Structural Features of Waxy Starches<sup>a</sup>

starch	amylose content (%)	degree of branching (%)	% starch chains of:						$\beta_1$	$\beta_2$	2/1	$X_{\text{min}2}$	crystallite type	A- or B-type crystallites (%)	V-type crystallites (%)	lamella HWHM (nm)	avg repeat distance (nm)
			$6 \leq X \leq 12$	$13 \leq X \leq 24$	$25 \leq X \leq 36$	$X \geq 37$											
EH-6 (wheat)	2.08 ± 0.09	4.5 ± 0.2	44.1	40.0	9.6	6.3	0.108	0.079	0.0251	12	A	40.0 ± 0.45	0.15 ± 0.09	1.78 ± 0.01	10.32 ± 0.04		
Eliane (potato)	0.51 ± 0.3	3.29 ± 0.04	33.3	41.1	12.1	13.5	0.091	0.062	0.0637	9	B	51.6 ± 9.3	1.12 ± 0.10	1.09 ± 0.03	9.15 ± 0.01		
F97 2-1 (sorghum)	1.34 ± 0.002	4.13 ± 0.09	43.1	41.8	9.3	5.9	0.107	0.082	0.0259	10	A	34.3 ± 1.6	0.37 ± 0.34	1.346 ± 0.004	9.52 ± 0.01		
Kiaryo-Mochi (rice)	0.4 ± 0.3	4.17 ± 0.03	45.3	39.3	8.9	6.5	0.112	0.077	0.0333	9	A	42.0 ± 0.2	0.22 ± 0.04	1.4 ± 0.01	9.52 ± 0.02		
Mazaca (maize)	0.06 ± 0.07	3.88 ± 0.02	40.1	41.9	10.6	7.4	0.099	0.073	0.0283	11	A	50.6 ± 1.6	0.22 ± 0.09	1.97 ± 0.01	10.6 ± 0.01		
Pulut-Siding (tice)	0.5 ± 0.3	4.20 ± 0.02	45.6	38.7	9.1	6.6	0.112	0.078	0.0328	10	A	25.39 ± 0.08	0.53 ± 0.12	1.5 ± 0.1	9.8 ± 0.1		
Shizuki-Mochi (tice)	0.3 ± 0.4	4.26 ± 0.02	46.1	39.1	8.8	6.1	0.111	0.078	0.0301	10	A	34.4 ± 1.1	0.12 ± 0.01	1.52 ± 0.01	9.69 ± 0.01		
W64A (maize)	3.06 ± 0.04	4.00 ± 0.12	41.0	42.4	10.1	6.5	0.108	0.08	0.0292	11	A	29.05 ± 0.76	0.63 ± 0.01	1.8 ± 0.05	10.34 ± 0.04		
Waxiro (barley)	10.15 ± 0.07	4.07 ± 0.05	46.1	39.1	8.8	6.1	0.107	0.078	0.0232	12	A	30.9 ± 3.1	0.75 ± 0.01	1.85 ± 0.02	10.34 ± 0.01		
waxy sorghum	2.7 ± 0.5	4.18 ± 0.08	41.0	42.3	9.8	6.9	0.111	0.079	0.0338	11	A	34.4 ± 4.1	0.09 ± 0.01	1.41 ± 0.02	9.59 ± 0.03		
YRW4 (rice)	2.5 ± 0.6	4.13 ± 0.06	46.1	39.1	8.8	6.1	0.114	0.077	0.032	9	A	37.8 ± 1.3	0.15 ± 0.05	1.41 ± 0.01	9.477 ± 0.002		

<sup>a</sup>Uncertainties in  $\beta_1$  and  $\beta_2$  are ±0.001.

and represent the variations in the number of chains when compared to the reference starch, Kiaryo-Mochi. The results show an effect of the botanical origin on the differences observed. The rice starches (Shizuki-Mochi, YRW4, and Pulut-Siding) display a similar pattern of difference. The sorghum starches (waxy sorghum and F97 2-1) are similar to Mazaca and W64A. Although Waxiro is a barley starch and EH-6 a wheat starch, they both show a similar difference pattern. The B-type starch, Eliane, shows little similarity with the other starches and displays a radically different difference plot from those of the other starches, showing a large increase in the number of chains above  $X \sim 16$ . This result is expected due to the observed correlation between B-type crystalline polymorphs and increases in the length of starch chains.<sup>26,39–41</sup>

The four divisions of the number distribution show relatively constant values within the different regions. The only sample which differs obviously in any of the regions is the B-type starch, which has fewer branches with DP in the range 6–12 and more above 25.

**Biosynthesis-Based Analysis.** An acceptable fit for the first enzyme set for all of the A- and B-type starches was produced using the similar values for the minimum DPs for branching enzyme to operate,<sup>21</sup>  $X_{\min 1}$  and  $X_0$ . The fitting parameters  $\beta_1$ ,  $\beta_2$ , and  $X_{\min 2}$  do not display any obvious correlations with different crystalline polymorphs. There is a large decrease in the 2/1 ratio seen between the B-type starch when compared to the values seen in the A-type starches; this is expected, as there is a large increase in the large number of long chains in B-type compared to A-type starches, and the long chains are formed by the second enzyme set. The full list of the parameters used for the fitting is given in the SI. The fitted  $N_{de}(X)$  from the biosynthesis-based model is very similar to experiment, and thus could be divided into the same four regions as the sub-divisional method (see SI).

The SAXS data for all starches exhibit a low- $q$  power law decay of the approximate form  $q^{-2}$ , with the expected broad peak centered around  $\sim 0.07 \text{ \AA}^{-1}$ .<sup>11</sup> These data are given in Figure 4, highlighting the lamellar region. The crystalline and crystalline–amorphous lamella structural parameters are shown in Table 1. The average repeat distance is within the range 9–10.5 nm, as observed for a variety of botanical species using a variety of fitting methods.<sup>8,9,18</sup>

The wide-angle X-ray scattering patterns are given in Figure 5 and show that all of the waxy starches display an A-type scattering pattern, with the exception of Eliane (waxy potato), which displays B-type crystallinity. The proportion of V-type crystallinity is low, as expected from waxy starches, as there is very little amylose content to generate the inclusion complexes that form V-type crystallites. The proportions of A- and B-type crystallinity vary significantly with botanical origin, with the rice starches typically displaying less crystallinity than the maize starches; significant variation is also observed between individual starch samples, which is readily seen between rice starches. A similar range of crystalline contents was found by Lopez-Rubio et al.<sup>34</sup> using the same crystal-defect fitting model.

Figure 6 contains plots of the two lamellar properties studied in the starches against two of the CLD structural parameters: the proportion of DP 6–12 chains and  $\beta_1$ . In these plots, a grouping of starches by botanical origin is apparent. The potato starch Eliane is distinct from the other starches, which is probably related to its B-type crystalline polymorph displaying radically different properties to that of other A-type crystallites. The sorghum samples also appear separate from the other

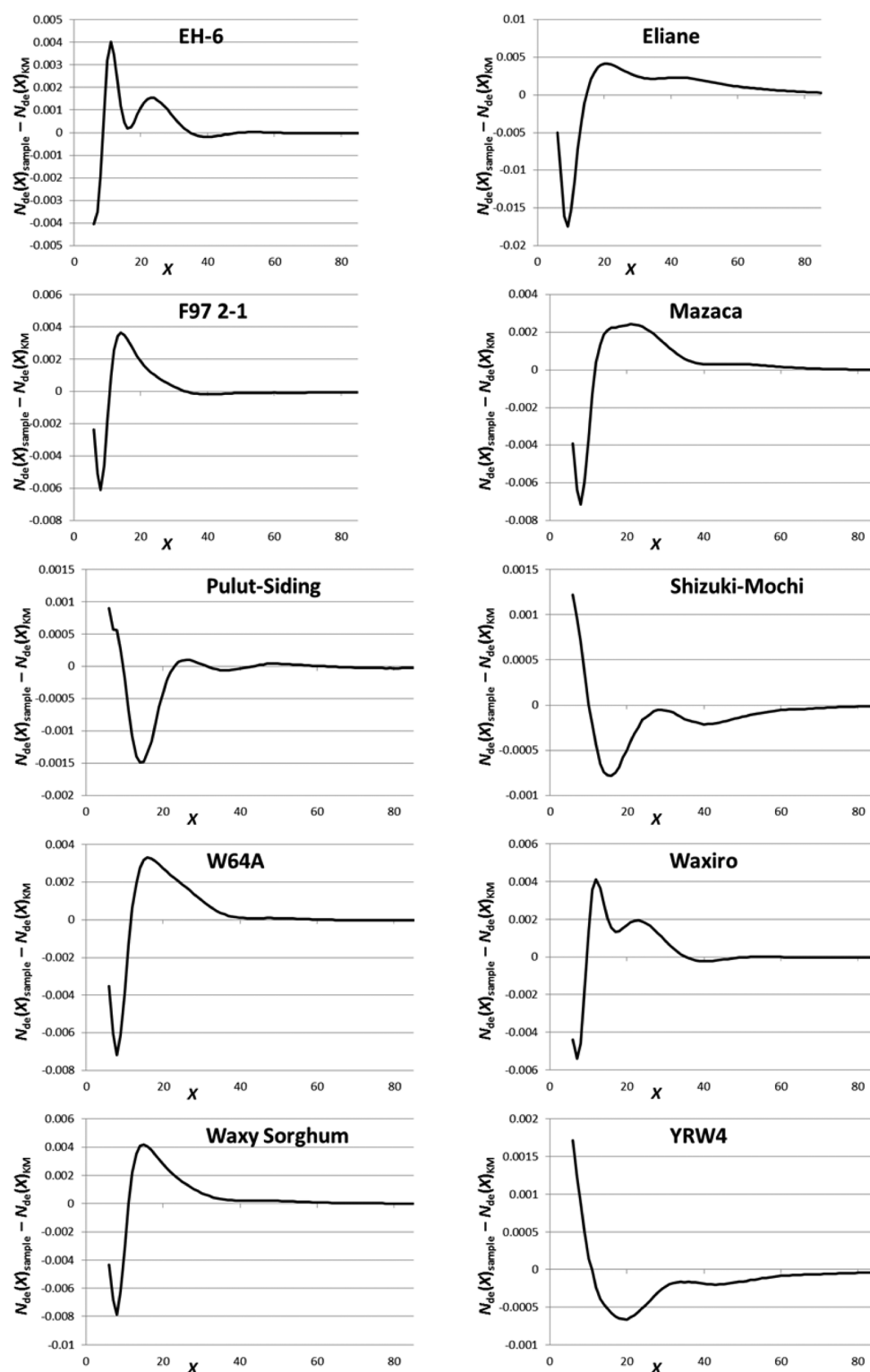


**Figure 3.** Number distribution difference plots using Kiaryo–Mochi (“KM”) as the reference starch, obtained via SEC.

starches, most clearly demonstrated in the DP 6–12 plots, which show the other rice, maize, wheat, and barley starches in a linear pattern with a negative slope. The pattern exhibited by the average repeat distance and HWHM plotted against the proportion of DP 6–12 chains is similar, with the only qualitative differences being the position of the four rice starches; this pattern similarity is also observed in the  $\beta_1$  plots. This indicates that both the average repeat distance and HWHM are affected

similarly by the short starch branches of the CLD, implying a correlation in these parameters. The HWHM and average repeat distance are plotted against all of the other CLD parameters in the SI, where a note is made of the parameters that do not appear linked.

**Statistics.** The visual comparison of the relationship between the lamellar properties and the CLD properties suggests some variation due to botanical origin. To account for the strong effect

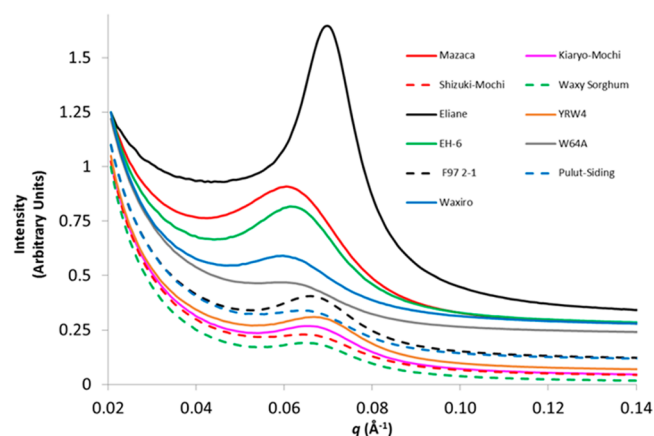


**Figure 4.** Small-angle X-ray scattering pattern of waxy starch, focused on the  $q$  region that is dominated by lamellar structure. Data have been shifted vertically for clarity.

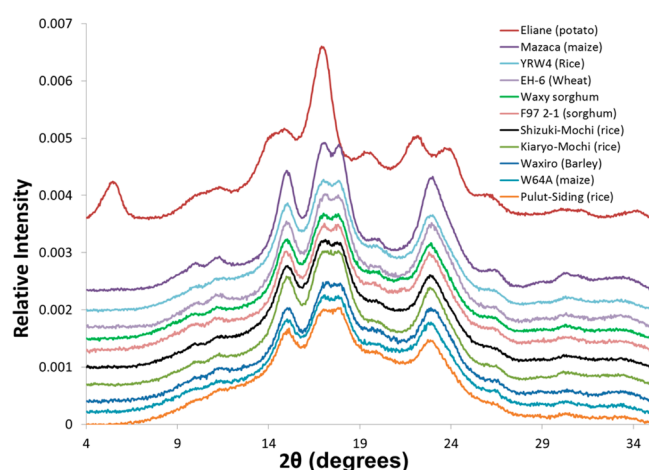


**Figure 5.** XRD patterns of waxy starches. Data have been shifted for clarity and are ordered from top to bottom.

of possible outliers in the statistical analysis, it was necessary to perform the statistics on four different groups of samples which separate the different botanical effects. These analyses are shown in Table 2, split into the following botanical groups: the correlations with all starches; the A-type starches after removing the B-type potato starch; and the correlations after removing the sorghum starches from the A-type starches; the correlations of only the four rice samples was also tested, but there were few correlations due to the small number of samples and the similarity of the rices' lamellar properties. While there are significant correlations between the different CLD parameters, they are omitted, as little useful information is obtained from comparing the two different analysis methods.

The positive correlation between the HWHM and the average repeat distance is constant, both in correlation and significance, regardless of the botanical varieties included in the study, indicating that this relationship occurs regardless of any other differences. Additionally, parameters that correlate with the average repeat distance also correlate with HWHM, with only small differences in the strength and significance of the correlations. A possible explanation for this is that the distribution of lamellar sizes in native starches displays a largely conserved distribution with a minimum allowed size. The minimum size limit is explained by the inability of starch chains smaller than a DP

of 10–12 to form helices, thus, interfering with crystallinity;<sup>42</sup> this will limit the production of the crystallites in the crystalline region and, thus, the size of the crystalline–amorphous lamellae. Thus, any increase in the ability to form larger lamellae, through either an increase in the size of the amorphous or crystalline components, will cause an increase in the width of the distribution of the lamellae and, without any change in the minimum lamellar size, an increase in the average repeat distance. Due to the direct correlation between the average repeat distance and HWHM in all cases, they will henceforth be referred to as lamellar size.

There are three other correlations that are constant, regardless of the botanical varieties analyzed: the negative correlation between  $\beta_2$  and A-/B-type crystallinity, the positive correlation between  $X_{\min 2}$  and lamellar size, and the negative correlation between  $2/1$  and lamellar size.  $\beta_1$  and  $\beta_2$  define the slope of the number distribution of starch after the main maximum and after the shoulder, respectively; larger values of  $\beta$  give a steeper slope and, thus, decrease the relative number of long compared to short chains. This reduction in longer chains may affect the production of crystallites in two ways: the reduction in the number of chains long enough to produce crystallites<sup>42</sup> and in the production of a greater variety of different lengths of starch chain,<sup>43</sup> both of which are known to inhibit the production of crystallites.

The parameter  $2/1$  is the relative contribution of each enzyme set, as shown in Figure 1. As such it is a good indicator of the proportion of the starch chains which are part of the shoulder and the longer chains.  $X_{\min 2}$  is the main parameter which defines the length of the shoulder and the beginning of the negative linear slope of the CLD. These two parameters are negatively correlated and together can be used to infer the size and length of the shoulder in the CLD. The negative correlation implies that as  $X_{\min 2}$  increases, the length of the shoulder in the CLD, the relative size of the shoulder ( $2/1$ ) and the second component in general is decreased. The relative decrease in shoulder size/prominence leads to a decrease in lamellar size, while an increase in length of the shoulder increases lamellar size.

Further correlations with the lamellar size become apparent when the diversity of botanical origin is taken into account in the statistical analysis. A negative correlation between  $\beta_1$  and lamellar size is seen in all cases in which the B-type potato starch is excluded. The subdivision parameters correlate with lamellar size when observing correlations not including the potato or sorghum starches; the positive correlations are between DP 13–24 and more strongly for DP 25–36 and lamellar size, and the negative correlation between DP 6–12 and lamellar size. Adding the other botanical varieties to the statistical analysis reduces the number of subdivision correlations observed: removing only potato leaves, the positive correlation between DP 25–36 and lamellar size is the only significant correlation, while no correlations are observed when examining all the starches. There are no correlations with the degree of branching, which would indicate that the average chain length of the amylopectin is not a significant factor in controlling the lamellar structure.

Two possible causes for the differences in subdivision correlations seen when factoring in the differences in botanical origin are as follows: either that different features are observed by the subdivisional dependence on botanical origin or that there are differences in the effect of the CLD in starches on the lamella structure depending on botanical origin. The subdivisional analysis may not include all of the important structural features consistently, such as the position of the maximum or the shoulder; this

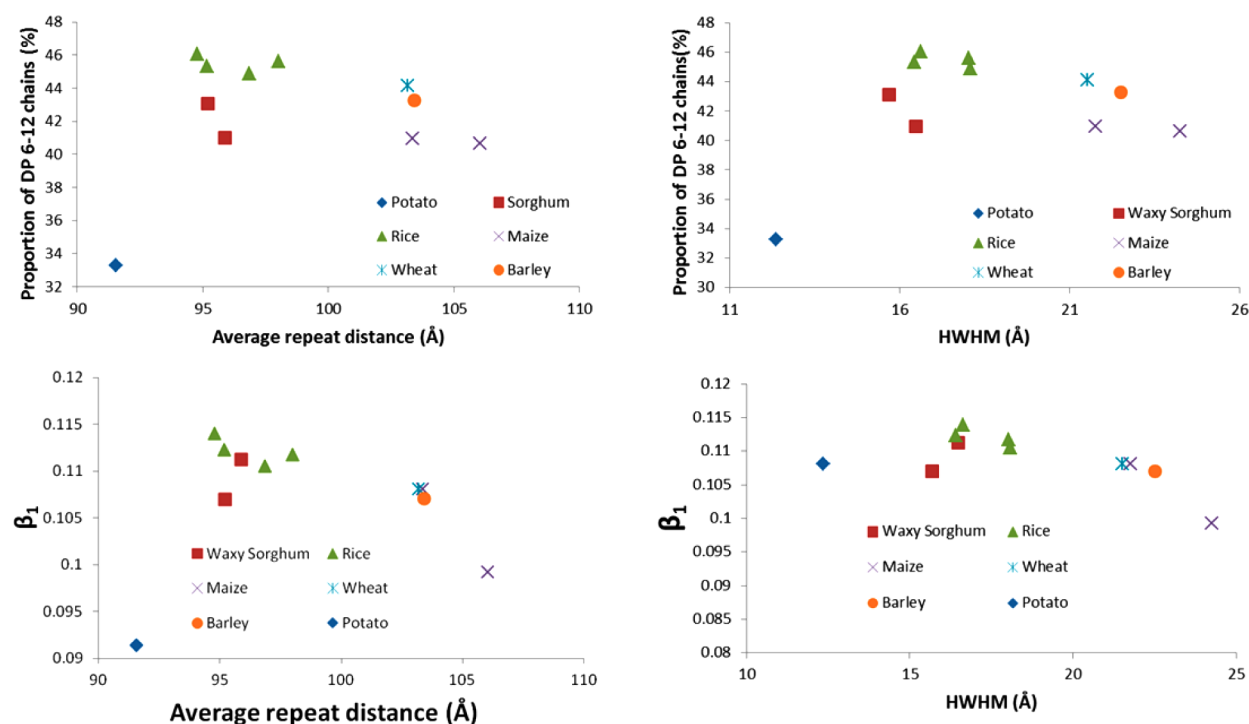


**Figure 6.** Comparison of the effect of botanical origin on the relationship between chain-length distribution (proportion of DP 6–12 chains and  $\beta_1$ ) and lamellar properties (average repeat distance and HWHM).

can change from starch to starch, which may change the subdivision in which they reside. The other option is that the effect of the different subdivisional regions changes from starch to starch, that is, the changes in the subdivision may not wholly describe the changes in lamellar structure. For example, the DP 6–12 subdivision may always correlate negatively with lamellar size in all starches, but the strength of that correlation may change between different species, leading to a loss of correlation when observing multiple species. This loss of correlation is observed in the biosynthetic parametrization as well, as the correlations between  $\beta_1$  and the lamellar size are only apparent when the potato starch is removed. However, the biosynthetic parametrization is less affected, as the  $X_{\min 2}$  and 2/1 correlations with lamella structure remain regardless of botanical origin. This lends weight to the idea that it is not the inability of the subdivisional parametrization to describe the CLD that is the cause of the changes in correlations with the addition of different botanical varieties. The changes in the effect of the CLD on the lamellar structure can be rationalized as arising from differences in the biosynthesis of the starch that do not relate to the CLD, such as differing moisture content or other physical conditions during synthesis between different species. Another potential cause is the action of other enzymes not related to the production of the starch molecules which modify the aggregation of starch chains, which would not be observed using the current enzyme sets.

The difference in the effect of the DP 6–12 chains and the DP 13–24 and  $\geq 37$  chains on the lamellar size is due to the inability of the smaller DP 6–12 chains to aggregate into double helices, necessary for the formation of the crystalline–amorphous lamellae.<sup>39,42</sup> All the other chain lengths are sufficient in size to produce the aggregate structures that allow the formation of the crystalline–amorphous lamellae. The importance of the shoulder of the CLD for the production of crystalline–amorphous lamellae of a greater size is probably due to their ability

to produce disordered chains beyond the crystalline regions and into the amorphous regions.<sup>25,35,44,45</sup> As the DP of the shoulder increases, the number of chains that extend beyond the crystalline region into the amorphous region increases and the size of the amorphous region increases; increases in the relative height of the shoulder, which causes a shortening of the shoulder length, leads to the opposite: a decrease in the amount of chains in the amorphous region and a decrease in lamellar size.

The increasing proportion of long chains in the slope of the CLD, manifest in the values of  $\beta_1$ , correlates with an increase in lamellar size. The change in size is probably due to the larger proportion of longer chains which are able to produce greater lengths of longer crystalline components in the crystalline lamellae. This then allows the increase in the lamellar size to be separated into two components: those that make the shoulder more pronounced and increase the number of disordered ends, thereby increasing the amorphous regions in size, and those that increase the proportion of long chains that allow the formation of longer crystalline regions.

Of the two different analysis methods, the subdivisional analysis is seen to provide less information and has been seen to be significantly more susceptible to the differences in botanical origin, as observed by the significant changes to the correlations observed when varying the number of different botanical varieties. The biosynthesis-based analysis is seen to provide information about the manner in which the structural features, such as the maximum, the shoulder, and the linear regions of the CLD, change the lamellar and crystalline properties of the starch. Moreover, the biosynthesis-based analysis is capable of fitting more accurate CLD data, which can be obtained using fluorophore-assisted carbohydrate electrophoresis, with additional isoform-sets perhaps enabling further structural insight.<sup>32</sup>

Noda et al.<sup>46</sup> studied the effect of a severe distortion of the structure of amylopectin in sweet potato. The “quick sweet”

Table 2. Pearson Correlation Coefficients for Three Starch Categories<sup>a</sup>

	avg repeat distance			HWHM		proportion of A-/B-type crystals			proportion of V-type crystals			
	all starch	A-type starch	A-type no sorghum	all starch	A-type starch	A-type no sorghum	all starch	A-type starch	A-type no sorghum	all starch	A-type starch	A-type no sorghum
level 3												
avg repeat distance				0.987 (0)	0.989 (0.00)	0.991 (0.00)						
HWHM	0.987 (0.00)	0.989 (0.00)	0.991 (0.00)									
proportion of A-/B-type crystals												
proportion of V-type crystals												
levels 1 and 2	$\beta_1$		−0.770 (0.01)	−0.885 (0.00)	−0.751 (0.01)	−0.913 (0.00)	−0.700 (0.02)			−0.599 (0.07)	−0.669 (0.07)	
	$\beta_2$						−0.745 (0.01)	−0.695 (0.03)	−0.799 (0.02)			−0.656 (0.03)
	2/1	−0.63 (0.038)	−0.589 (0.07)	−0.747 (0.03)	−0.692 (0.02)	−0.568 (0.09)	−0.767 (0.03)	0.530 (0.09)				−0.608 (0.05)
	$X_{\min 2}$	0.818 (0.002)	0.778 (0.01)	0.881 (0.00)	0.778 (0.00)	0.730 (0.02)	0.864 (0.01)					0.602 (0.05)
	DP 6-12			−0.875 (0.00)			−0.881 (0.00)	−0.563 (0.07)				−0.670 (0.02)
	DP 13-24			0.793 (0.02)			0.803 (0.02)					
	DP 25-36		0.808 (0.00)	0.954 (0.00)		0.771 (0.01)	0.958 (0.00)	0.605 (0.05)			0.696 (0.02)	
	DP $\geq 37$							0.631 (0.04)			0.694 (0.02)	
degree of branching							−0.549 (0.08)			−0.759 (0.01)		
amylose fraction										0.635 (0.05)	0.737 (0.04)	

<sup>1</sup>  $p$  values in parentheses, with only significant ( $p \leq 0.05$ ) or possibly significant ( $0.05 < p \leq 0.1$ ) listed.



variety had 150% as many short amylopectin branches (DP 6–12) compared to a normal variety of sweet potato. There was a radical decrease in the total amount of crystallinity, the proportion of crystalline regions within the lamellar structure, the average size of the lamellar repeat, and a decrease in thermodynamic parameters, including enthalpy and melting temperature, related to the size of crystalline melting unit. This is in agreement with the current results that the lamellar repeat distance decreases with an increase in short chains. However, the current results are focused on waxy A-type starches, while the Noda et al. study involved different crystallite structures in the two starches investigated, one being a predominately A-type starch and the other a C-type starch; further comparisons between the two studies are therefore not possible.

Sanderson et al.<sup>9</sup> studied the relationship between different starches using small-angle X-ray scattering, interpreting the data with the modified paracrystalline model of Daniels et al.,<sup>12,47</sup> and measured amylopectin chain lengths from high performance anion exchange chromatography (HPAEC) with pulsed amperometric detection. Due to the use of the different SAXS model, and because HPAEC suffers from a mass bias,<sup>48</sup> a direct comparison between this and the present study is not attempted here. Sanderson et al. note that they are able to separate the A-, B-, and C-type starches on the basis of CLD and lamellar properties. However, the CLD results are assigned arbitrarily into five DP subdivisions without a consideration of mechanistically relevant correlations.

As noted by an anonymous reviewer, only about half the amylopectin in a grain is in the amorphous–crystalline lamellae, with the rest located elsewhere in the amorphous region of the growth rings. However, while the level 3 characterization techniques (SAXS, XRD) probe the lamellae, the level 1 technique, SEC, gives a CLD, which is an average over the whole sample. There is the possibility that the CLD of amylopectin in the lamellae might be significantly different from that elsewhere in the grain, which would call the correlations seen here into question. However, this possibility is very unlikely, for the following reasons. (1) The observed strong correlations between CLD and lamellar properties obtained are completely consistent with the same amylopectin CLD being in both locations. (2) There is evidence to show that there is a single CLD for a specific population of amylopectin molecules regardless of the size of the whole amylopectin molecules,<sup>49</sup> and there is no reason to suppose that the whole amylopectin molecules would have the same size in all locations. (3) There is little or no change observed in the CLD of amylopectin at different times of the day/night cycle of transient starch production, which implies that, at least in the case of leaf starch, there is conservation of the amylopectin CLD during synthesis.<sup>50</sup>

## CONCLUSION

This study reveals correlations between two levels of starch structure: the amylopectin CLDs (parametrized by two alternative methods), proportion of crystallinity and the size and distribution of the crystalline–amorphous lamellae in a group of 11 predominantly waxy A-type starches. This gives the first direct mechanistic link between high-level (crystalline–amorphous lamellar) structural features and low-level (amylopectin chain length) structures in waxy starch; it also implies some limit on any differences in amylopectin molecular structure based upon location in the granule. An increase in the proportion of the shortest amylopectin branches decreases the average repeat distance and width distribution (HWHM) of the

crystalline–amorphous lamellae, probably by reducing the number of the larger crystalline lamellae. All longer chain lengths, DP 13–24 and  $\geq 25$ , increase the average repeat distance and HWHM; however, the extent of this is heavily affected by the botanical origins of the starch. The importance of the position and size of the shoulder observed in the CLD has a strong effect on the lamellar size, probably by increasing the size of the amorphous region as the number of chains that produce disordered ends at the end of starch crystallites and enter the amorphous region.<sup>35,44,49,50</sup> The proportion of longer chains within the slope regions of the CLD is important and is probably due to an increase in the production of larger crystalline lamellae, this is further reinforced by the positive correlation between the slope of the second enzyme set and the proportion of A- and B-type crystallinity. The biosynthesis-based analysis proved to be more able to encapsulate the structural features of the CLD of starches, displaying less variation with botanical origin and providing more meaningful information.

There is some indication that, while there are underlying effects of the chain length of amylopectin upon the higher structural order of starch, there is also some indication that the extent to which the amylopectin structure affects the lamellar structure is based on the botanical origin of the starch. This suggests that while level 1 structure (chain-length distribution) largely controls the high-level crystalline structure, there may also be some effect on the production of lamellar structure beyond simple enzymatic control of branching, such as some enzymatic “shepherding” of the crystallization process or differences in synthesis conditions due to botanical origin.

## ASSOCIATED CONTENT

### Supporting Information

Fitting parameters used in the Wu–Gilbert model, comparison to the experimental CLD, and comparison using the subdivision parametrization; fitting parameters to the SAXS data; comparison between degree of branching calculations of <sup>1</sup>H NMR and SEC; comparison of botanical origin plots; Spearman correlation coefficients; botanical origins of the samples. This material is available free of charge via the Internet at <http://pubs.acs.org>.

## AUTHOR INFORMATION

### Corresponding Author

\*Fax: +61 7 3365 1188. Tel.: +61 7 3365 4809. E-mail: [b.gilbert@uq.edu.au](mailto:b.gilbert@uq.edu.au)

### Notes

The authors declare no competing financial interest.

## ACKNOWLEDGMENTS

We gratefully acknowledge the Australian Institute of Nuclear Science and Engineering for a PGRA Grant (T.W.) and the help of Dr. Bernadine Flanagan in the processing of XRD data. The authors would also like to thank CSIRO Plant Industry, DPI Yanco Agricultural Institute, DEEDI (all in Australia), and MARDI (Malaysia) for providing samples.

## REFERENCES

- (1) Putaux, J. L.; Cardoso, M. B.; Dupeyre, D.; Morin, M.; Nulac, A.; Hu, Y. *Macromol. Symp.* **2008**, 273, 1–8.
- (2) Pérez, S.; Bertoft, E. *Starch/Stärke* **2010**, 62, 389–420.
- (3) Popov, D.; Buléon, A.; Burghammer, M.; Chanzy, H.; Montesanti, N.; Putaux, J. L.; Potocki-Véronèse, G.; Riekkel, C. *Macromolecules* **2009**, 42, 1167–1174.

- (4) Imberty, A.; Chanzy, H.; Perez, S.; Buleon, A.; Tran, V. J. *Mol. Biol.* **1988**, *201*, 365–78.
- (5) Takahashi, Y.; Kumano, T.; Nishikawa, S. *Macromolecules* **2004**, *37*, 6827–6832.
- (6) Imberty, A.; Perez, S. *Biopolymers* **1988**, *27*, 1205–21.
- (7) Buleon, A.; Colonna, P.; Planchot, V.; Ball, S. *Int. J. Biol. Macromol.* **1998**, *23*, 85–112.
- (8) Jenkins, P. J.; Cameron, R. E.; Donald, A. M. *Starch/Stärke* **1993**, *45*, 417–20.
- (9) Sanderson, J. S.; Daniels, R. D.; Donald, A. M.; Blennow, A.; Engelsens, S. B. *Carbohydr. Polym.* **2006**, *64*, 433–43.
- (10) Cameron, R. E.; Donald, A. M. *Polymer* **1992**, *33*, 2628–2636.
- (11) Blazek, J.; Gilbert, E. P. *Biomacromolecules* **2010**, *11*, 3275–3289.
- (12) Daniels, D. R.; Donald, A. M. *Macromolecules* **2004**, *37*, 1312–1318.
- (13) Cardoso, M. B.; Westfahl, H., Jr. *Carbohydr. Polym.* **2010**, *81*, 21–28.
- (14) Blazek, J.; Gilbert, E. P. *Carbohydr. Polym.* **2011**, *85*, 281–293.
- (15) Douth, J.; Gilbert, E. P. *Carbohydr. Polym.* **2013**, *91*, 444–451.
- (16) Donald, A. M.; Kato, K. L.; Perry, P. A.; Weigh, T. A. *Starch/Stärke* **2001**, *53*, 504–512.
- (17) Jenkins, P. J.; Donald, A. M. *Starch/Stärke* **1997**, *49*, 262–267.
- (18) Douth, J.; Bason, M.; Franceschini, F.; James, K.; Clowes, D.; Gilbert, E. P. *Carbohydr. Polym.* **2012**, *88*, 1061–1071.
- (19) Tester, R. F.; Debon, S. J. *Int. J. Biol. Macromol.* **2000**, *27*, 1–12.
- (20) Gomand, S. V.; Lamberts, L.; Gommès, C. J.; Visser, R. G. F.; Delcour, J. A.; Goderis, B. *Biomacromolecules* **2012**, *13*, 1361–1370.
- (21) Wu, A. C.; Gilbert, R. G. *Biomacromolecules* **2010**, *11*, 3539–3547.
- (22) Srichuwong, S.; Sunarti, T. C.; Mishima, T.; Isono, N.; Hisamatsu, M. *Carbohydr. Polym.* **2005**, *60*, 529–538.
- (23) Jane, J.; Chen, Y. Y.; Lee, L. F.; McPherson, A. E.; Wong, K. S.; Radosavljevic, M.; Kasemsuwan, T. *Cereal Chem.* **1999**, *76*, 629–637.
- (24) Srichuwong, S.; Isono, N.; Jiang, H.; Mishima, T.; Hisamatsu, M. *Carbohydr. Polym.* **2012**, *87*, 1275–1279.
- (25) Koroteeva, D. A.; Kiseleva, V. I.; Krivandin, A. V.; Shatalova, O. V.; Blaszcak, W.; Bertoft, E.; Piyachomkwan, K.; Yuryev, V. P. *Int. J. Biol. Macromol.* **2007**, *41*, 534–547.
- (26) Hanashiro, I.; Abe, J.; Hizukuri, S. *Carbohydr. Res.* **1996**, *283*, 151–159.
- (27) Hasjim, J.; Lavau, G. C.; Gidley, M. J.; Gilbert, R. G. *Biomacromolecules* **2010**, *11*, 3600–3608.
- (28) Vilaplana, F.; Gilbert, R. G. *J. Sep. Sci.* **2010**, *33*, 3537–3554.
- (29) Vilaplana, F.; Gilbert, R. G. *Macromolecules* **2010**, *43*, 7321–7329.
- (30) Cave, R. A.; Seabrook, S. A.; Gidley, M. J.; Gilbert, R. G. *Biomacromolecules* **2009**, *10*, 2245–2253.
- (31) International Standardization Organization Determination of Amylose Content. *ISO 6647-2*, 2011.
- (32) O'Shea, M. G.; Samuel, M. S.; Konik, C. M.; Morell, M. K. *Carbohydr. Res.* **1998**, *307*, 1–12.
- (33) Tizzotti, M. J.; Sweedman, M. C.; Tang, D.; Schaefer, C.; Gilbert, R. G. *J. Agric. Food Chem.* **2011**, *59*, 6913–6919.
- (34) Lopez-Rubio, A.; Flanagan, B. M.; Gilbert, E. P.; Gidley, M. J. *Biopolymers* **2008**, *89*, 761–768.
- (35) Blazek, J.; Salman, H.; Rubio, A. L.; Gilbert, E.; Hanley, T.; Copeland, L. *Carbohydr. Polym.* **2009**, *75*, 705–711.
- (36) Fan, L. X.; Degen, M.; Bendle, S.; Grupido, N.; Ilavsky, J. The Absolute Calibration of a Small-Angle Scattering Instrument with a Laboratory X-ray Source. In *XIV International Conference on Small-Angle Scattering*; Ungar, G., Ed.; Iop Publishing Ltd.: Bristol, 2010; Vol. 247.
- (37) Ilavsky, J.; Jemian, P. R. *J. Appl. Crystallogr.* **2009**, *42*, 347–353.
- (38) Kline, S. R. *J. Appl. Crystallogr.* **2006**, *39*, 895–900.
- (39) Pfannemüller, B. *Int. J. Biol. Macromol.* **1987**, *9*, 105–108.
- (40) Cheetham, N. W. H.; Tao, L. *Carbohydr. Polym.* **1997**, *33*, 251–261.
- (41) Kubo, A.; Yuguchi, Y.; Takeniasa, M.; Suzuki, S.; Satoh, H.; Kitamura, S. *J. Cereal Sci.* **2008**, *48*, 92–97.
- (42) Gidley, M. J.; Bulpin, P. V. *Carbohydr. Res.* **1987**, *161*, 291–300.
- (43) Montesanti, N.; Véronèse, G.; Buléon, A.; Escalier, P.-C.; Kitamura, S.; Putaux, J.-L. *Biomacromolecules* **2010**, *11*, 3049–3058.
- (44) Kiseleva, V. I.; Krivandin, A. V.; Fornal, J.; Blaszcak, W.; Jelinski, T.; Yuryev, V. P. *Carbohydr. Res.* **2005**, *340*, 75–83.
- (45) Yuryev, V. P.; Krivandin, A. V.; Kiseleva, V. I.; Wasserman, L. A.; Genkina, N. K.; Fornal, J.; Blaszcak, W.; Schiraldi, A. *Carbohydr. Res.* **2004**, *339*, 2683–2691.
- (46) Noda, T.; Isono, N.; Krivandin, A. V.; Shatalova, O. V.; Blaszcak, W.; Yuryev, V. P. *Carbohydr. Polym.* **2009**, *76*, 400–409.
- (47) Daniels, D. R.; Donald, A. M. *Biopolymers* **2003**, *69*, 165–175.
- (48) Koch, K.; Andersson, R.; Aman, P. *J. Chromatogr., A* **1998**, *800*, 199–206.
- (49) Vilaplana, F.; Gilbert, R. G. *J. Chromatogr., A* **2011**, *1218*, 4434–4444.
- (50) Delatte, T.; Trevisan, M.; Parker, M. L.; Zeeman, S. C. *Plant J.* **2005**, *41*, 815–830.